

Synthesis and Characterization of ZnO Semiconductor Nanoparticles with Annealing Temperature Variation for Dye Synthesized Solar Cell Application

Article Info

Article history :

Received October 09, 2023
Revised August 02, 2024
Accepted August 05, 2024
Published September 30, 2024

Keywords :

Annealing, ZnO,
gel-combustion, chlorophyll,
nanoparticle

Idawati Supu^{1*}, Aulia Fitrah Ramadhani¹, Bunga Tang¹,
Haerul Ahmadi¹, Dewa Gede Eka Setiawan¹

¹Department of Physics, Faculty of Mathematics and Natural Science, Universitas Negeri Gorontalo, Gorontalo, Indonesia

Abstract. This study aims to make ZnO semiconductor nanoparticles using annealing temperature variations for dye synthesized solar cells, identify the structure and particle size and surface morphology using SEM-EDX and UV-VIS to determine the wavelength and absorbance values. In the *gel-combustion* method, three samples were made with varying annealing temperatures of 700°C, 800°C, and 900°C, respectively. The annealing temperature variation shows the difference in SEM test results, where the higher the annealing temperature, the smaller the particle size. EDX test results show that ZnO has been formed. In the UV-VIS characterization results for the three samples have different transmittance values and wavelengths from samples without dye, ZnO doping chlorophyll. Based on XRD data, the higher the calcination temperature, the smaller the particle size, and the distribution of particle size at each increase in annealing temperature. Based on the results of SEM analysis obtained that the particle size is getting smaller with increasing annealing temperature. According to the UV-Vis analysis results obtained that the addition of chlorophyll extract does not have a significant effect about wavelength 370 nm on the transmittance value of each sample, so the best absorbance is owned by the ZnO doping dye sample.

This is an open access article under the [CC-BY](https://creativecommons.org/licenses/by/4.0/) license.



This is an open access article distributed under the Creative Commons 4.0 Attribution License, which permits unrestricted use, distribution, and reproduction in any medium, provided the original work is properly cited. ©2024 by author.

Corresponding Author :

Idawati Supu
Department of Physics, Faculty of Mathematics and Natural Science,
Universitas Negeri Gorontalo, Gorontalo, Indonesia
Email : idawatisupu@ung.ac.id

1. Introduction

Indonesia has very significant energy needs along with the times so that the availability of fossil energy is decreasing. Humans need electrical energy which is a type of primary energy. The depletion of fossil energy has made researchers think about how to make electrical energy available without having to use fossil energy [1-2]. The discovery of a device that can be converted from solar energy into electrical energy [3-4]. Humans need energy for survival. The use of fossil energy in the long run can cause the supply of energy sources to run out. One of the alternative energy sources in Indonesia is sunlight. Professor Michael Gratzel (2003) first developed DSSC (*Dye Sensitized Solar Cell*). This DSSC functions to convert solar energy into electrical energy [5].

DSSC is one of the potential candidate solutions for future solar cells, because it does not have to use high purity materials so that the production process costs are lower. The difference with conventional solar cells is that all processes involve silicon material, DSSC light absorption and electrical charge separation occur in separate processes. Light absorption is done by dye molecules, and charge separation by inorganic semiconductor nanocrystals that have a wide band gap [6]. Semiconductors with wide band gaps expand electrons flowing from the conduction band to the valence band, with a wide band gap that will make the photocatalyst reaction space and absorption by the dye will become more or in other words the absorption spectrum becomes wide [7-8].

Research in recent years began to be carried out with a biological approach in synthesizing nanoparticles, one of the ways that some researchers have done using plant extracts as the best alternative method that is environmentally friendly when compared to other methods [9-10]. In this study, a natural dye from Moringa leaf extract was used. It has been researched that the flesh in moringa leaves is obtained green pigments whose absorbance in the visible wavelength range so that it can be used as a dye in DSSC (Dye Sensitized Solar Cell) efficiency. Besides being easier to obtain, the materials used in this study have a much more economical cost [11-12]. Moringa leaf itself was chosen as a natural chlorophyll dye because it has the highest chlorophyll content and is easily obtained.

ZnO (Zinc Oxide) is a type-n semiconductor with 3.37 eV as its band gap and 60 MeV as its binding energy. ZnO is a material that is widely used and applied in solar cells, laser diodes, ultraviolet lasers, thin films, piezoelectric transducers, and gas sensors [8]. Semiconductors are between insulators and conductors. In semiconductor materials, the conduction band and valence band play an important role. The band gap is also called the distance between the conduction band and the valence band [1].

ZnO semiconductor nanoparticles are generally in the form of powders, toxic properties and high thermal stability, direct band gap with material width of 3.37 eV and strong ultra-violet (UV) emission. This is influenced by the high exciton bond energy of 60 MeV at room temperature, which is much higher than gallium nitride 25 MeV [1]. The low-temperature hydrothermal-sonochemical method produces ZnO nanostructures. Ultrasonic time can also enlarge the crystal size range. The ZnO samples synthesized by ultrasonic process for 30 minutes gave optimal results with purity and crystallinity and quite good and smaller size range. It is necessary to analyze the sample through other characterizations to obtain more accurate information on the ZnO nanostructure obtained [3].

There were many methods in improving synthesis ZnO likes made it be nanorods a hedgehog-like structure by hydrothermal method. One of the properties of ZnO nanoparticles that is considered is heat treatment, namely annealing. Increasing the annealing temperature affects the number of grains, dye absorbance ability, and current density. The annealing process is the process of heating the material to a certain temperature. Then the process is held for some time and then cooling is carried out slowly in the furnace. The advantages obtained from this process include; reducing hardness, improving mechanical properties, reducing or eliminating structural inhomogeneity, and refining grain size. Variations in annealing temperature during synthesis can affect the particle size, thus indirectly affecting the crystal size [6-8].

The purpose of this research is to make ZnO semiconductor nanoparticles using annealing temperature variations for dye-synthesized solar cell (DSSC) applications, see the surface morphology of ZnO nanoparticles using SEM-EDX, and to know the absorbance value and wavelength and distribution of crystal size and strain of ZnO semiconductor.

2. Experimental Section

2.1. Materials

The equipment used in the preparation and synthesis stages of semiconductor materials to dye coating include: a set of Nabertherm furnaces, glassware, electric heaters, Ohaus Pioneer PX423/E analytical balance, MSH-300i magnetic stirrer, Phenom ProX Scanning Electron Microscopy (SEM), and Orion AquaMate 8000 UV-Vis Spectrophotometer. The materials used in this study include: zinc acetate dihydrate ($\text{Zn}(\text{CH}_3\text{COO})_2 \cdot 2\text{H}_2\text{O}$) p.a Merck product, citric acid ($(\text{C}_6\text{H}_7\text{O}_8) \text{H}_2\text{O}$) p.a Merck product, distilled water, preparation glass, PEG 400, ethanol, and natural dye from Moringa oleifera leaf extract.

2.2. Tips

2.2.1 Synthesis Nanoparticles ZnO

Three samples were made by weighing the solid $\text{Zn}(\text{CH}_3\text{COO})_2 \cdot 2\text{H}_2\text{O}$ using an analytical balance and then dissolved with 50 ml of distilled water in a 100 mL beaker for each sample to form a ZnO solution with a solubility set at 0.3 mol/Liter [13-14]. Then citric acid solution was made by taking citric acid solids into a beaker and then weighed using an analytical balance of 40 grams. The solid was then dissolved with distilled water as much as 18.75 ml. The citric acid solution formed was then transferred into a volumetric flask.

The ZnO solution was transferred into a beaker and then placed on an electric heater while stirring using a stirring rod for less than 1 hour. Then the solution was stirred for approximately 2 hours using a magnetic stirrer on a hot plate with a maximum temperature of 120°C, heating is done gradually to get a uniform solution and evaporate the solvent. During the stirring process, 10 drops of citric acid solution were added to the ZnO solution using a dropper pipette every 5 minutes. When the water solvent completely evaporates, a gel phase will form. The beaker containing the 3 samples was then covered using aluminum foil and allowed to stand overnight and then dried using an oven.

Each sample was then crushed and transferred to a porcelain cup to be burned using a furnace. For the first sample, the furnace was set with the initial condition of burning at a maximum temperature of 200°C for 30 minutes where the gel will expand and form like foam. This situation is called self-propagating combustion reaction to obtain powder material. Then the furnace temperature is gradually increased to reach a maximum temperature of 500°C within 3 hours, where annealing conditions will be obtained. After the temperature reaches 500°C, the combustion is stabilized for 1 hour. The next stage is the final combustion, where the temperature is gradually increased to reach a maximum temperature of 700 °C within 3 hours. After reaching 700°C, the furnace temperature is lowered to 100°C, then turned off and after a while the sample can be removed.

For the second sample, the furnace tool is set with the initial condition of burning at a maximum temperature of 300 ° C for 30 minutes where the gel will expand and form like foam. Then the furnace temperature is gradually increased to reach a maximum temperature of 600°C within 3 hours, where annealing conditions will be obtained, then the combustion is set to stabilize for 1 hour. In the final stage, the temperature is gradually increased to reach a maximum temperature of 800°C within 3 hours. The furnace temperature is lowered to 100°C, then turned off and after a while the sample can be removed.

For the third sample, the furnace tool is set with the initial condition of burning at a maximum temperature of 400 °C for 30 minutes where the gel will expand and form like foam. Then the furnace temperature is gradually increased to reach a maximum temperature of 700°C within 3 hours, where

annealing conditions will be obtained, then the combustion is set to stabilize for 1 hour. In the final stage, the temperature is gradually increased to reach a maximum temperature of 900°C within 3 hours. The furnace temperature is lowered to 100°C, then turned off and after a while the sample can be removed.

2.2.2 ZnO Semiconductor Coating Casting Method

a. ZnO Coating without Dye

Each ZnO sample was weighed using an analytical balance of 0.017 grams then mixed and mashed with 3 drops of polyethylene glycol 400 (PEG 400) using a mortar and pestle. The sample was then dripped on the preparation glass and coated with the casting method. The coated samples were then dried on a hot plate at 74°C. After drying, each sample will be characterized by UV-Vis spectrophotometer [15].

b. ZnO Coating with Chlorophyll Dye

Each ZnO sample was weighed using an analytical balance of 0.017 grams then mixed and mashed with 3 drops of polyethylene glycol 400 (PEG 400) and chlorophyll dye (*Moringa oleifera* extract) using a mortar and pestle. The sample was then dripped on a glass plate and coated with the casting method. Samples that have been coated are then dried by aerating. After drying, each sample will be characterized by UV-Vis spectrophotometer [16].

2.2.3 Measurement of Morphology, Crystallinity and Optical Properties of Film

a. X-Ray Diffraction Characterization

Crystallinity, phase type, density and structure tests were carried out using X-Ray Diffraction (XRD) crystallography tools, in this section 3 samples were tested based on temperature variations and running at 2θ angles of 20° to 80°.

b. SEM Characterization and EDX Test

Morphological structure analysis was carried out using a Phenom ProX G5 Desktop SEM (Scanning Electron Microscope). The sample is placed on a pin stub that has been attached to adhesive carbon tape, then the sample is sprayed to remove light particles that may stick. The next, the sample was coated using a sputter coater with the target material used, Au/Pd. The sample was then coated for 60 seconds at a current of 20 mA. Then the sample was inserted into the SEM using a 12.1 mm distance SE detector with 10 kV ETH.

c. UV-Vis Characterization

UV-Vis spectrophotometry is the interaction that occurs between energy in the form of monochromatic light from a light source with material in the form of molecules. The amount of energy absorbed is certain and causes electrons to be excited from the ground state to an excited state that has higher energy.

3. Results and Discussion

In Figure 1 XRD characterization results were obtained on ZnO samples at annealing temperatures of 700°C, 800°C, 900°C. Based on Figure 1, the XRD characterization results show that the phase formed remains the same despite variations in the annealing temperature. However, the intensity of each peak varies, indicating that the ZnO structure formed is crystalline. Increasing the annealing temperature has a significant impact on changes in the crystal structure of the ZnO sample, where the higher the annealing temperature, the higher the crystallinity of the ZnO sample formed. The phase seen in the image shows the wurtzite phase. Based on confirmation from JCPDS data, all peaks that appear correspond to the ZnO phase, with no other peaks that do not correspond to ZnO.

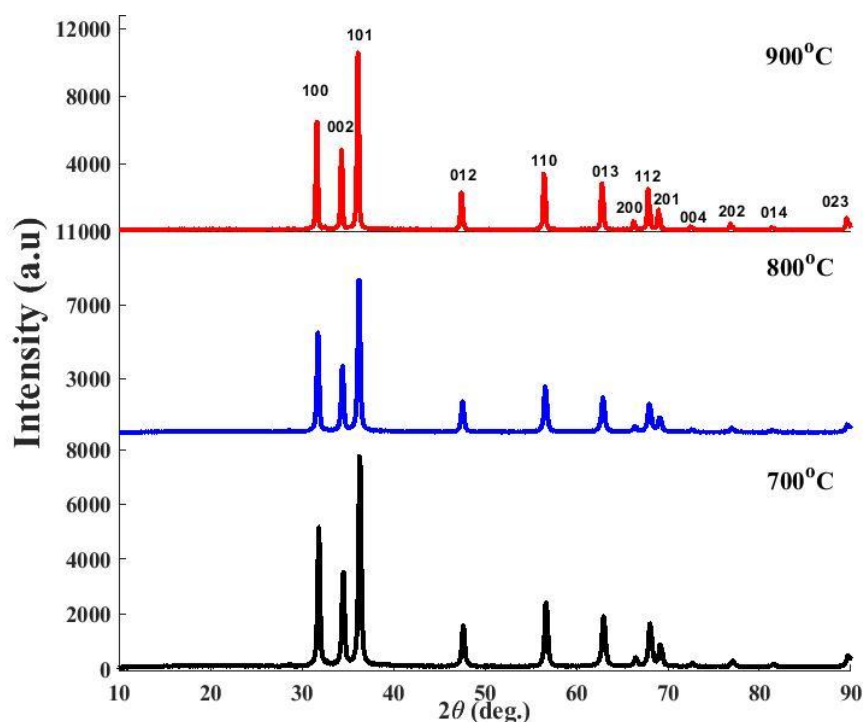


Figure 1. X-Ray Diffraction Analysis Results on ZnO at annealing temperature 700°C, 800°C, 900°C

These results are consistent with the theory of crystal growth, which states that higher annealing temperatures tend to increase atomic diffusion, allowing atoms in the material to find lower and more stable energy positions, which in turn increases crystallinity. This theory explains that at higher annealing temperatures, atoms in ZnO are better able to rearrange themselves in a more regular crystal structure, which is detected as an increase in peak intensity in the XRD results [17-18].

The wurtzite phase identified in the ZnO sample is also in accordance with the literature stating that the wurtzite crystal structure is the most stable form of ZnO at high temperatures. The JCPDS data confirming the presence of only the ZnO peak confirms that the dominant phase formed is the wurtzite phase, without any other phases or contaminants [19].

In addition, the variability of the XRD peak intensity at different annealing temperatures can be related to the theory that the size of the crystalline domain or crystal texture is also affected by the thermal conditions during the annealing process. This difference in intensity indicates that the annealing temperature not only affects the degree of crystallinity but also may affect the crystal orientation or domain size in the sample [20].

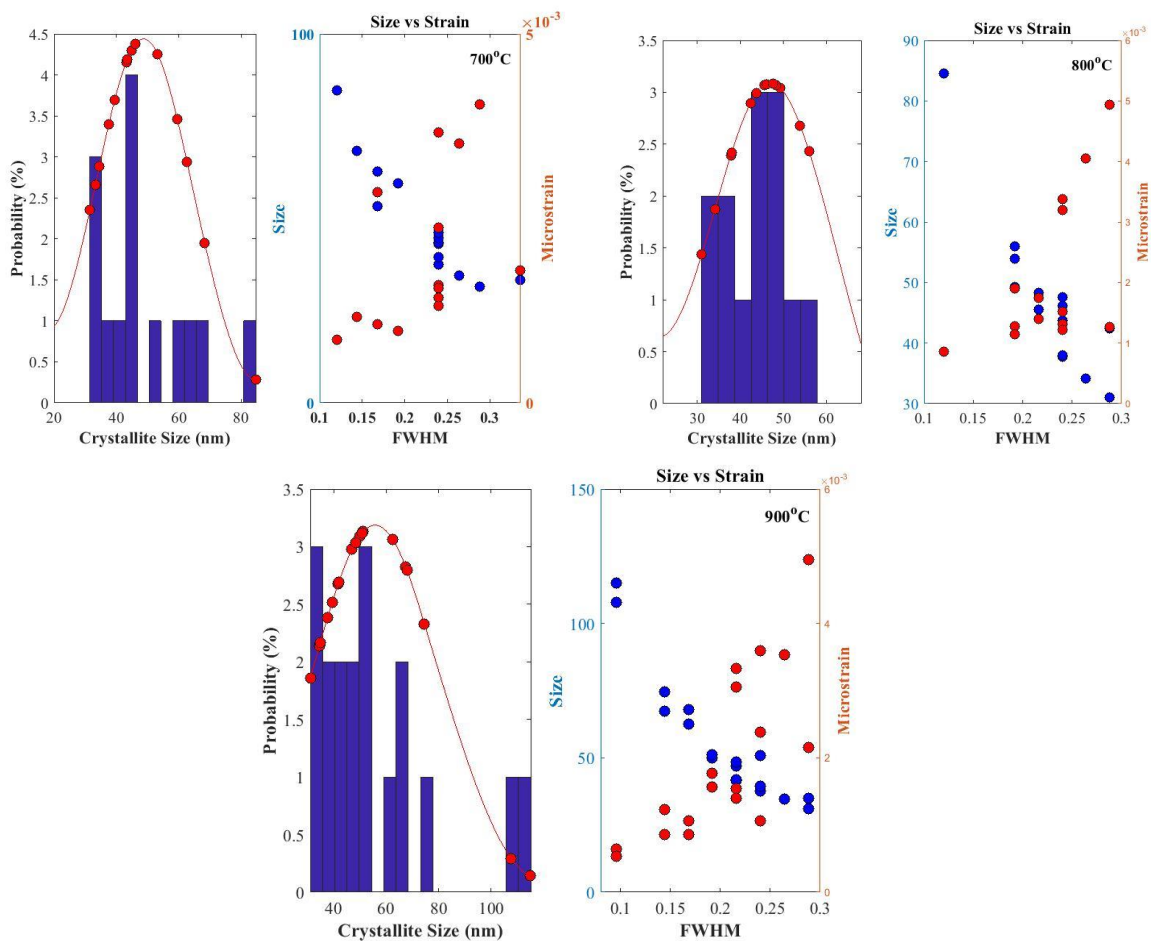


Figure 2. Crystal size distribution and strain of ZnO at 700°C, 800°C, 900°C

Based on Figure 2, the crystallite size distribution at each temperature is different. At 700°C, the crystallite size ranges from 30-60 nm, with a sparser size distribution compared to the distribution shown in 800°C, which tends to be denser. This sparser distribution provides a greater opportunity for nanoparticle grain growth at the nucleation stage. The higher the calcination temperature, the greater the energy given to the atoms during the diffusion process, so that a smaller surface will experience a greater increase in energy.

These results are in line with the grain growth theory and the atomic diffusion theory in crystalline materials. At higher calcination temperatures, the thermal energy transferred to the atoms in the material increases, which causes the atoms to move more easily (diffusion) and find lower energy sites, allowing for more significant grain growth [21-22].

Diffusion theory explains that at higher temperatures, atoms in the material are more thermally active, which accelerates their diffusion process. This explains why at 700°C, larger grain sizes tend to form. The looser size distribution at 700°C suggests that the nucleation and crystal growth processes are more dynamic and allow for larger size variations, which is expected in the early stages of crystal formation when diffusion energy still significantly influences crystal structure formation. In contrast, at 800°C shows a tighter crystal size distribution, which is likely because at lower temperatures, the thermal energy available for atomic diffusion is lower, allowing for more controlled and uniform grain growth.

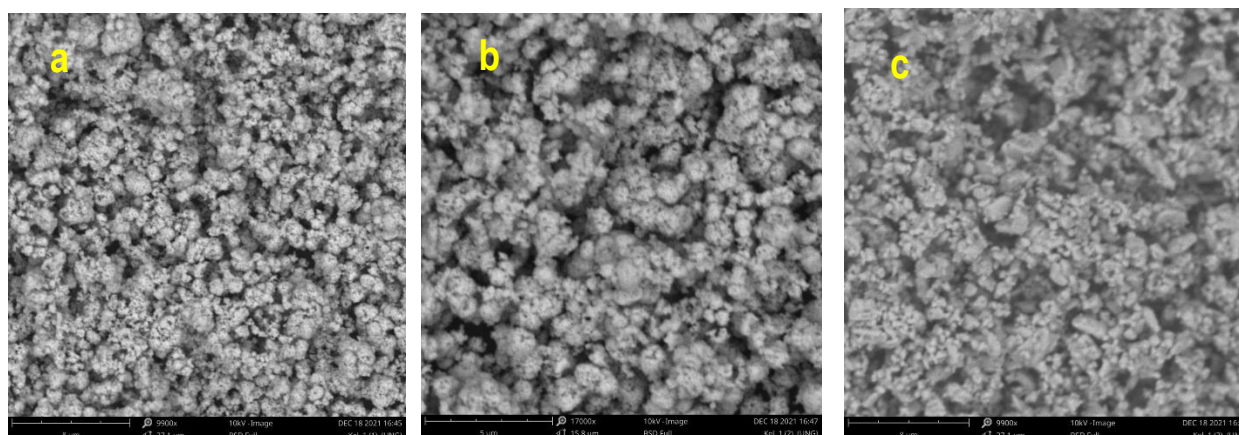


Figure 3. SEM of annealed samples at temperature at 700°C (a), 800°C (b), 900°C (c).

Scanning Electron Microscope (SEM) testing in magnification about 9900x was conducted to determine the morphology and particle size of the ZnO layer. Testing undoped samples, there are three temperature variations including 700 °C, 800 °C, and 900 °C. In Figure 3 tends to have a particle size with a distribution of 3.25%. which provides a high opportunity for grain growth.

The SEM test results of the first sample showed a heterogeneous particle shape with an average particle size of 1.125 μm . There is still agglomeration between particles. Figure 3(b) shows the SEM test results for the second sample, where agglomeration between particles still occurs. The particle shape is also still heterogeneous with an average particle size of 835.5 nm. Figure 3(c) presents the SEM characterization results of the third sample. In the last sample, the smallest particle size was obtained, with an average of 679.6 nm. The third sample particles are also still agglomerated and some of the shapes are still heterogeneous.

Based on the SEM characterization results for the three samples, it can be seen that the largest particle size is owned by the first sample with annealing temperatures of 700 °C and 800 °C. While the smallest particles are owned by the third sample with the highest annealing temperature, 900°C annealing temperature. The particles in each sample are still agglomerated due to the poor citric acid dripping process, where the synthesis process is carried out directly instead of gradually. In addition, the temperature during the heating process on the hot plate must also be increased gradually. The grinding of samples that have passed the combustion process with a furnace is also not optimal so that the particle size obtained is still large even though it is nano-sized. Analysis of the atomic composition of ZnO thin films using EDX aims to determine the atomic percent composition of the atoms that make up the coating [23-24]. EDX test results show that the constituents of ZnO thin film are Zinc (Zn) and Oxygen (O).

Table 1. EDX test results of sample 1 at annealing temperature of 700 °C

Element Number	Element Symbol	Element Name	Atomic Conc.	Weight Conc.
30	Zn	Zinc	34.16	67.85
8	O	Oxygen	65.79	31.97

Table 1 shows the EDX test results for the first sample, where the weight percent for zinc is higher than that for oxygen. When summed up, the total weight percent for zinc and oxygen does not reach 100%. This is because there are still impurities obtained from less sterile tools in the synthesis process.

Table 2. EDX test results of sample 1 at annealing temperature of 800 °C

Element Number	Element Symbol	Element Name	Atomic Conc.	Weight Conc.
30	Zn	Zinc	38.59	71.97
8	O	Oxygen	61.41	28.03

Based on Table 2, the weight percent of the second sample is also dominated by zinc with 71.97%. Table 3 shows that the weight percent of zinc is also more than the weight percent of oxygen. The total weight percent of zinc and oxygen is 100%.

Table 3. EDX test results of sample 1 at annealing temperature of 900 °C

Element Number	Element Symbol	Element Name	Atomic Conc.	Weight Conc.
30	Zn	Zinc	44.11	76.33
8	O	Oxygen	55.89	23.67

These results can be explained by the theory of material composition and the influence of contamination on chemical composition analysis. In the context of material synthesis, ideally the chemical composition detected by EDX (Energy Dispersive X-ray Spectroscopy) test reflects the pure chemical composition of the material being synthesized [25-26]. However, if the equipment or synthesis environment is not completely sterile, contamination can occur, resulting in the detection of elements that should not be present in the sample.

In the first sample (Table 1), the contamination detected can be explained by the theory that impurities or the presence of foreign elements can affect the measurement of chemical composition. When the total weight percentage of the expected elements (zinc and oxygen) does not reach 100%, this indicates that other elements may be present, but are not detected or are in amounts too small to be identified by EDX, or that there is a problem in the data collection process.

In contrast, Table 3 shows results that are in accordance with the theory of material composition, where the total weight percentage of zinc and oxygen reaches 100%. This indicates that this sample is purer and free from significant contamination, allowing the detection of elements that correspond to the expected chemical composition.

In Table 2, the dominance of zinc at 71.97% can also be explained by the stoichiometry theory, which shows that the proportion between zinc and oxygen in ZnO compounds can vary depending on the synthesis conditions, such as temperature and partial pressure of oxygen during the formation of the material.

Based on Figure 4, it is obtained that the increase in calcination temperature results in a lower transmittance value. This occurs because when energy enters the sample more fraction of energy is absorbed compared to that which is forwarded, as a result the fraction of energy that is forwarded becomes smaller. However, the transmittance value for the 800°C sample is lower than the 900°C sample which has the highest temperature. The low transmittance value can be influenced by the thickness and roughness of the resulting film. The thicker and rougher the film, the lower the transmittance value.

This shows the relationship between wavelength and transmittance for each sample without doping. Based on the graph, it can be seen that at 370 nm, the sample with a calcination temperature of 900°C has the highest transmittance value, followed by the sample with a calcination temperature of 700°C and the sample with a calcination temperature of 800°C. Then in this range, an unstable increase in percent transmittance is obtained for all samples. However, the transmittance value of the 700°C sample experienced the most drastic increase to surpass the other samples with a transmittance of 58%.

The decrease in transmittance values with increasing calcination temperature suggests that at higher temperatures, the film may have become thicker or undergo changes in its microstructure that increase the absorption of light energy. This is consistent with the theory that increasing the calcination temperature can increase grain growth, which can cause the film to become denser and rougher, thus decreasing transmittance [27-28].

However, the anomaly seen in the 800°C sample—where the transmittance value is lower than at 900°C—suggests that other factors may be at play, such as differences in thickness or surface irregularities that may have occurred during the calcination process. The theory of light-material interactions suggests that surface roughness and irregularities can cause greater light diffusion, reducing the amount of light transmitted. The drastic change in the transmittance values of the samples at 700°C may reflect the optimal conditions where the film has a better combination of thickness, roughness, and grain distribution, allowing more light to be transmitted at a given wavelength.

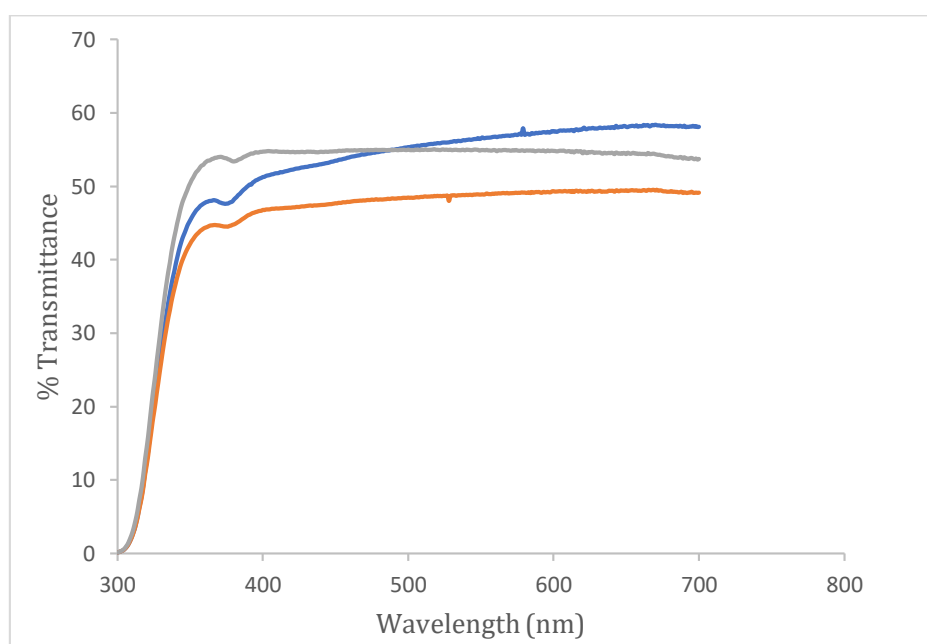


Figure 4. Graph without chlorophyll dye addition at each temperature 700°C —, 800°C —, 900°C —

Based on Figure 5, it is obtained that the increase in calcination temperature results in a lower transmittance value. This occurs because when energy enters the sample more fraction of energy is absorbed compared to that which is forwarded, as a result the fraction of energy that is forwarded becomes smaller. However, the transmittance value for the 800°C sample is lower than the 900°C sample which has the highest temperature. The low transmittance value can be influenced by the thickness and roughness of the resulting film. The thicker and rougher the film, the lower the transmittance value.

The decrease in transmittance with increasing calcination temperature suggests that the material undergoes microstructural changes that increase light absorption. At higher temperatures, grain growth in the material can cause the film to become thicker and rougher, which in turn increases the amount of light absorbed and reduces transmittance. This is consistent with the theory that thicker and rougher materials will absorb more light and inhibit transmission [29-30].

However, the anomaly seen in the 800°C sample, where the transmittance is lower than the 900°C sample, suggests that there may be additional factors influencing these results. One possibility is that at 800°C, there is greater nonuniformity in thickness or surface roughness, which increases light

diffusion and absorption, thereby reducing transmittance. Theories of diffraction and scattering of light by rough surfaces support this explanation, where greater surface roughness causes more light scattering, reducing the amount of light transmitted.

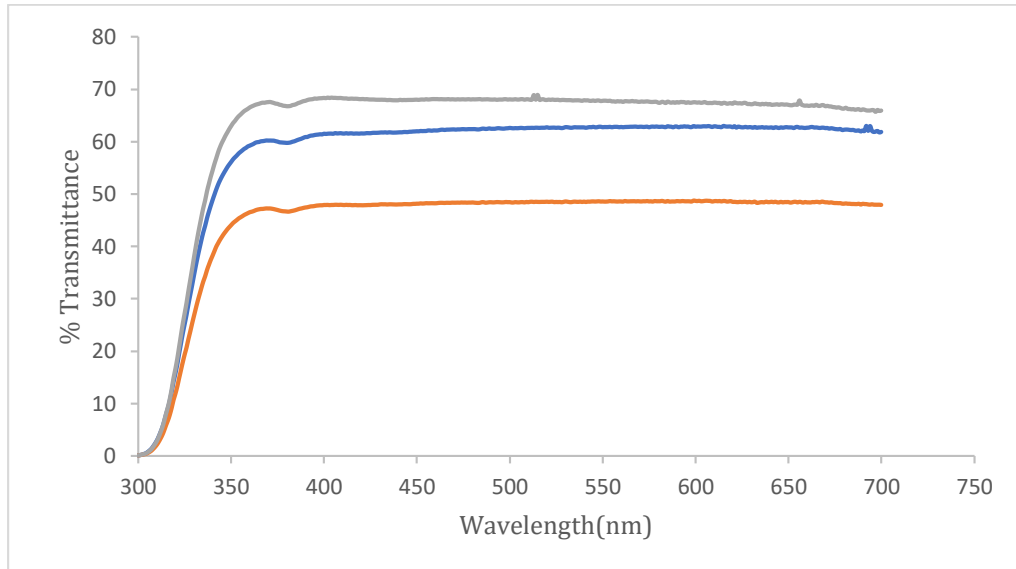


Figure 5. Graph with chlorophyll dye addition at each temperature 700°C —, 800°C —, 900°C —

4. Conclusion

The synthesis and preparation of ZnO semiconductor nanomaterials have been successfully carried out using the Gel-Combustion method with variations in annealing temperature. The composition of the nanomaterial based on EDX test results is zinc (Zn) and oxygen (O), which is dominated by zinc. SEM test results show that in each sample there is still agglomeration between particles, with the maximum nanoparticle size owned by sample 3 with the highest temperature (700 °C, 800 °C and 900 °C). Based on XRD data, it was found that the higher the calcination temperature, the smaller the particle size, and the particle size distribution at each increase in annealing temperature. Based on the results of SEM analysis, it is found that the particle size is getting smaller with increasing annealing temperature. The UV-Vis test results show that the addition of chlorophyll extract does not have a significant effect on the absorbance value of each sample, so the best transmittance is owned by the ZnO sample without doping dye.

References

- [1] Siagian, S. M. (2021). Analisis Semikonduktor zno: cu terhadap efisiensi dye Sensitized Solar cell menggunakan ekstrak alami. *Jurnal ELEMENTER (Elektro dan Mesin Terapan)*, 7(2), 51-57.
- [2] Tyona, M. D., Osuji, R. U., Ezema, F. I., Jambure, S. B., & Lokhande, C. D. (2015). Highly efficient natural dye-sensitized photoelectrochemical solar cells based on Cu-doped zinc oxide thin film electrodes. *Adv. Appl. Sci. Res*, 6, 7-20.
- [3] Oktaviani, Y. (2014). Sintesis Lapisan Tipis Semikonduktor dengan Bahan Dasar Tembaga (Cu) Menggunakan Chemical Bath Deposition. *Jurnal Fisika Unand*, 3(1).
- [4] Chaki, S. H., Deshpande, M. P., & Tailor, J. P. (2014). Characterization of CuS nanocrystalline thin films synthesized by chemical bath deposition and dip coating techniques. *Thin Solid Films*, 550, 291-297.

- [5] Ardianto, R., Nugroho, W. A., & Sutan, S. M. (2015). Uji Kinerja Dye Sensitized Solar Cell (DSSC) Menggunakan Lapisan Capacitive Touchscreen Sebagai Substrat dan Ekstrak Klorofil *Nannochloropsis* Sp. Sebagai Dye Sensitizer dengan Variasi Ketebalan Pasta TiO₂. *Journal of Tropical Agricultural Engineering and Biosystems-Jurnal Keteknik Pertanian Tropis dan Biosistem*, 3(3), 325-337.
- [6] Smith, A. M., & Nie, S. (2010). Semiconductor nanocrystals: structure, properties, and band gap engineering. *Accounts of chemical research*, 43(2), 190-200.
- [7] Nadaek, S. M., & Susanti, D. (2012). Variasi temperatur dan waktu tahan kalsinasi terhadap unjuk kerja semikonduktor TiO₂ sebagai dye sensitized solar cell (DSSC) dengan dye dari ekstrak buah naga merah. *Jurnal Teknik ITS*, 1(1), F81-F86.
- [8] Siregar, N. (2019). The Effect of Post-Heating Time of ZnO Thin Film on the Efficiency of ZnO *Hylocereus polyrhizus* DSSC. *Edelweiss Applied Science and Technology*, 3(1), 70-74.
- [9] Siddiqui, M. H., Al-Whaibi, M. H., & Mohammad, F. (2015). Nanotechnology and plant sciences. *Springer International Publishing Switzerland. DOI*, 10, 978-3.
- [10] Sanzari, I., Leone, A., & Ambrosone, A. (2019). Nanotechnology in plant science: to make a long story short. *Frontiers in Bioengineering and Biotechnology*, 7, 120.
- [11] Pinem, S. K. (2018). *Pengaruh Waktu Tahan Kalsinasi Film Tipis ZnO Terhadap Efisiensi DSSC (Dye Sensitized Solar Cell) Yang Menggunakan Dye dari Buah Naga Merah* (Doctoral dissertation, UNIMED).
- [12] Wahyuono, R. A., Risanti, I. D. D., & Ihara, H. TITLE Dye-Sensitized Solar Cells (DSSC) Fabrication with TiO₂ and ZnO Nanoparticle for High Conversion Efficiency.
- [13] Ong, C. B., Ng, L. Y., & Mohammad, A. W. (2018). A review of ZnO nanoparticles as solar photocatalysts: Synthesis, mechanisms and applications. *Renewable and Sustainable Energy Reviews*, 81, 536-551.
- [14] Hong, R., Pan, T., Qian, J., & Li, H. (2006). Synthesis and surface modification of ZnO nanoparticles. *Chemical Engineering Journal*, 119(2-3), 71-81.
- [15] Vittal, R., & Ho, K. C. (2017). Zinc oxide based dye-sensitized solar cells: A review. *Renewable and Sustainable energy reviews*, 70, 920-935.
- [16] Haghighatzadeh, A. (2021). Visible-light-active chlorophyll/flavonoid-sensitized ZnO nanoparticles: preparation and optical and photocatalytic studies. *Journal of the Australian Ceramic Society*, 57(1), 137-147.
- [17] Jackson, K. A. (2010). *Kinetic processes: crystal growth, diffusion, and phase transitions in materials*. John Wiley & Sons.
- [18] Markov, I. V. (2016). *Crystal growth for beginners: fundamentals of nucleation, crystal growth and epitaxy*. World scientific.
- [19] Sharma, D. K., Shukla, S., Sharma, K. K., & Kumar, V. (2022). A review on ZnO: Fundamental properties and applications. *Materials Today: Proceedings*, 49, 3028-3035.
- [20] Verploegen, E., Mondal, R., Bettinger, C. J., Sok, S., Toney, M. F., & Bao, Z. (2010). Effects of thermal annealing upon the morphology of polymer–fullerene blends. *Advanced Functional Materials*, 20(20), 3519-3529.
- [21] Hu, J., Wang, X., Zhang, J., Luo, J., Zhang, Z., & Shen, Z. (2021). A general mechanism of grain growth— I. Theory. *Journal of Materiomics*, 7(5), 1007-1013.
- [22] Jackson, K. A. (2010). *Kinetic processes: crystal growth, diffusion, and phase transitions in materials*. John Wiley & Sons.
- [23] Sutanto, H., Nurhasanah, I., Hidayanto, E., & Arifin, Z. (2013). Deposisi Lapisan Tipis Foto Katalis Seng Oksida (ZnO) Berukuran Nano dengan Teknik Penyemprotan dan Aplikasinya untuk Pendegradasi Pewarna Methylene Blue. *Jurnal Fisika*, 3(1).

-
- [24] Pantò, F., Dahrouch, Z., Saha, A., Patanè, S., Santangelo, S., & Triolo, C. (2021). Photocatalytic degradation of methylene blue dye by porous zinc oxide nanofibers prepared via electrospinning: When defects become merits. *Applied Surface Science*, 557, 149830.
- [25] Newbury*, D. E., & Ritchie, N. W. (2013). Is scanning electron microscopy/energy dispersive X-ray spectrometry (SEM/EDS) quantitative?. *Scanning*, 35(3), 141-168.
- [26] Howarth, A. J., Peters, A. W., Vermeulen, N. A., Wang, T. C., Hupp, J. T., & Farha, O. K. (2017). Best practices for the synthesis, activation, and characterization of metal–organic frameworks. *Chemistry of Materials*, 29(1), 26-39.
- [27] Kumar, R., Kumar, G., Al-Dossary, O., & Umar, A. (2015). ZnO nanostructured thin films: Depositions, properties and applications—A review. *Materials Express*, 5(1), 3-23.
- [28] Wang, F. H., Chao, J. C., Liu, H. W., & Kang, T. K. (2015). Physical properties of ZnO thin films codoped with titanium and hydrogen prepared by RF magnetron sputtering with different substrate temperatures. *Journal of Nanomaterials*, 2015(1), 936482.
- [29] Zak, A. K., Hashim, A. M., & Esmailzadeh, J. (2024). Role of CeO₂ and calcination temperature on the structural and optical properties of (ZnO)_{1-x}/(CeO₂)_x nanocomposites in the UV–visible region. *Ceramics International*, 50(2), 4167-4177.
- [30] Massoudi, I., Ghrib, T., Al-Otaibi, A. L., Al-Hamad, K., Al-Malky, S., Al-Otaibi, M., & Al-Yatimi, M. (2020). Effect of yttrium substitution on microstructural, optical, and photocatalytic properties of ZnO nanostructures. *Journal of Electronic Materials*, 49, 5353-5362.